Photoinduced Charge Separation and Photovoltaic Properties of Polypyrrole Having Pendant Bipyridinium Electron Acceptor Groups

Y. Eichen,*,†,‡ G. Nakhmanovich,† O. Epshtein,‡,§ and E. Ehrenfreund‡,§

Department of Chemistry, Solid State Institute, and Department of Physics, Technion-Israel Institute of Technology, Haifa 32000, Israel

Received: August 9, 1999; In Final Form: November 12, 1999

The application of conjugated polymers having electroactive pendant groups, such as poly(*N*-methyl-*N*′-(3-pyrrol-1-ylpropyl)-4,4′-bipyridinium), p-Pyr-V^{2+}-Me, and poly(*N*-hydrogen-*N*′-(3-pyrrol-1-ylpropyl)-4,4′-bipyridinium), p-Pyr-V^{2+}-H, as active photovoltaic and photoconducting media is investigated. Photoinduced charged species are characterized using photomodulated differential transmission spectroscopy and photoconductivity. The ability of using such media as active layers in photovoltaic cells is demonstrated.

I. Introduction

Recent advances in the application of organic-based conjugated polymers in light-emitting diodes and as conductive and photoconductive media, promoted intensive research aimed at a better understanding of the photophysics and optoelectronic properties of such materials.[1] Of particular interest are photoinduced electron and energy transfer processes taking place between different polymer strands in solid solutions and blends[2] as well as between polymer strands and guest molecules,[3] or acceptor groups attached to the polymer backbone.[4] The motivation to explore the electrooptical characteristics of such materials arises from their possible applications in organic-based solar cells and light sensors. Various conjugated polymer systems were shown to undergo efficient photoinduced electron-transfer processes with different host molecules, such as quinones[5] and fullerenes.[3] Furthermore, mixed solutions of electron rich and electron poor polymers were shown to undergo photoinduced charge separation.[6] Stabilization of the charge-separated states against charge recombination was claimed to originate from delocalization of charges on large conjugated systems, such as the polymer backbone and fullerene skeleton.[7] Different factors, like the polarity of the medium, free energy difference between the redox pair and reorganization energy, were found to affect electron−hole pair generation efficiency and stability. Nevertheless, often material properties such as the morphology and effective donor−acceptor separation complicate the picture due to a lesser understanding of these factors.[8]

Ultrafast (τ < 1 ps) and highly efficient forward electron transfer processes were reported for systems of conjugated polymers in conjunction with electron acceptor groups, competing efficiently against the alternative radiative recombination process. The charge-separated states in such systems exhibit lifetimes as long as milliseconds.[9] However, once generated, electrons and holes exhibit asymmetry in mobility, since holes are usually located in the conjugated system while electrons remain localized on isolated electron acceptors.[3]

N,*N*′-Dimethyl-4,4′-bipyridinium (**1**, Me_2V^{2+}) moieties present some unique properties as electron acceptor units: (1) Most systems containing Me_2V^{2+} units exhibit two reversible redox processes, suitable for long-lived devices.[10] (2) The redox properties of Me_2V^{2+}-containing systems can be easily tuned by derivatization of the basic system at the *N*,*N*′, 3,3′, or 5,5′ positions.[11] Derivatization at these positions increases the steric hindrance in the system upon inter-ring planarization that follows reduction. (3) Monoreduced bipyridinium moieties, $Me_2V^{\bullet+}$, tend to dimerize and aggregate at high local concentrations.[12] The aggregation may result in improved mobility of the excess electrons normal to the pyridine ring planes. (4) The different redox states of Me_2V^{2+} have only a low oscillator strength for optical transitions in the 400−600 nm spectral range.

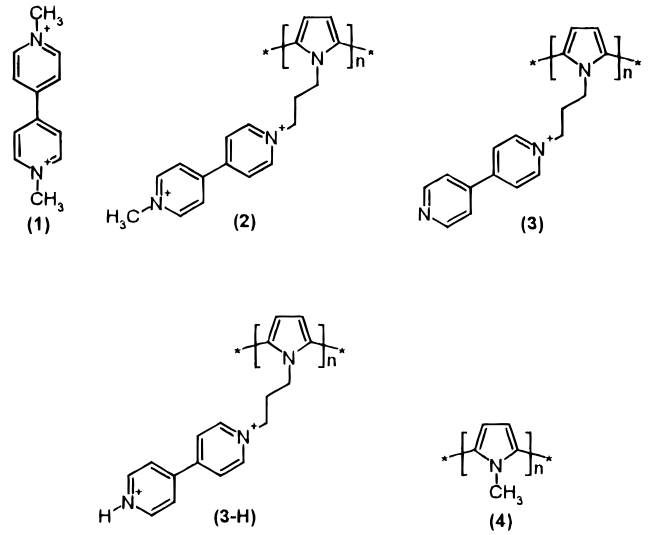

The application of conjugated polymers having electroactive pendant groups, such as poly(*N*-methyl-*N*′-(3-pyrrol-1-ylpropyl)-4,4′-bipyridinium) (**2**, p-Pyr-V^{2+}-Me) and poly(*N*-hydrogen-*N*′-(3-pyrrol-1-ylpropyl)-4,4′-bipyridinium) (**3**-H, p-Pyr-V^{2+}-H) for efficient charge separation and transport is of high interest as an alternative for heterogeneous systems composed of blends and solid solutions of electro-active mediators as dopants in conjugated polymer blends. Previously, the synthesis and electrochemical and redox processes with different chromophores were reported for polypyrroles having pendant

† Department of Chemistry.
‡ Solid State Institute.
§ Department of Physics.

10.1021/jp9927956 CCC: $19.00
Published on Web 01/11/2000

bipyridinium moieties and the generation of photocurrent was demonstrated in wet cells containing different sacrificial electron donors and photosensitizers.[13] Reversible redox processes and electron-transport properties of the reduced state of the polymer were also reported.[14] Such polymers were also applied as the electrical wiring of enzyme-electrode systems.[15]

Here we report on a detailed study on photoinduced charge separation, photoconductivity, and photovoltaic properties of p-Pyr-V^{2+}-Me and p-Pyr-V^{2+}-H in the solid-state. Photomodulated absorption measurements clearly show the photoinduced formation of long-lived charge-separated species. Electron−hole recombination processes obey bimolecular relaxation kinetics possibly due to high charge mobility relative to the lifetime of the charge-separated state. Photoconductivity and photovoltaic effects in an ITO|polymer|gold sandwich type device are characterized under steady-state illumination conditions.

II. Experimental Section

II.a. Materials and Samples. p-Pyr-V^{2+}-Me and p-Pyr-V^{2+}-H were prepared according to previously reported procedures.[16] Synthesis and analytical data regarding the different monomers and polymers are described in the Supporting Information.

Films for optical measurements (absorption, spectro-electrochemistry, and photoinduced absorption), photoconductivity, and cyclic voltammetry were prepared by electropolymerizing the appropriate monomers onto ITO-coated glass electrodes. Electropolymerization conditions: A solution of 30 mM of *N*-methyl-*N*′-(3-pyrrol-1-ylpropyl)-4,4′-bipyridinium dihexafluorophosphate or *N*-(3-pyrrol-1-ylpropyl)-4,4′-bipyridinium hexafluorophosphate and 0.1 M tetraethylammonium perchlorate in dry, deoxygenated, acetonitrile was electolyzed at +1.6 V vs saturated calomel electrode using ITO-coated glass or Pt as the anode. After dedoping, freshly prepared films were washed repeatedly with acetonitrile and then oven dried (70 C, 10^{-5} mmHg, 12 h). This procedure yielded reproducible and homogeneous 0.5−1 μm thick films, according to the specific polymerization conditions.

Films with varying concentrations of monoreduced bipyridinium species were obtained by first applying a bias of −0.6 V vs SCE and then turning off the bias and waiting for a few seconds in ambient atmosphere before measuring the spectrum again.

Films for photoconductivity measurements were prepared using a similar electropolymerization process followed by the deposition of counter gold electrodes (typically 1000 Å thick, 0.0625 mm^2) on the polymer film using standard CVD techniques. Gold contacts were welded to the devices using an ultrasonic wedge bonding machine (Kulicke and Soffa Industries, model 4123).

II.b. Apparatus. The film thickness was determined using an α-Step (Tencor Instruments, α-Step 200). Absorption spectra were measured on a UV1601 (Shimadzu) UV−visible spectrophotometer. Photoinduced absorption (PIA) measurements were recorded on a homemade spectrometer described elsewhere.[17] The PIA setup consists of an argon ion laser (Coherent, Innova 90C, λ = 350 nm + 360 nm) as the pump beam, and a 250 W xenon arc lamp (Oriel) or a 100 W tungsten lamp as the probe beam for the UV or vis, respectively. The probe light was analyzed using various detectors (covering the UV−vis−IR spectral range) attached to a monochromator (Jarrel-Ash, 0.25 m) equipped with a set of interchangeable gratings. Samples were mounted onto a cold finger cryostat (Air-Product, LT-3-1100) under vacuum. Transmission, *T*, and audio frequency photomodulated differential transmission (corrected for photoluminescence), ΔT, were recorded using a standard phase-sensitive lock-in setup. The ratio $-\Delta T/T$ is then the net change in the absorption due to the modulated pump light source.

SCHEME 1

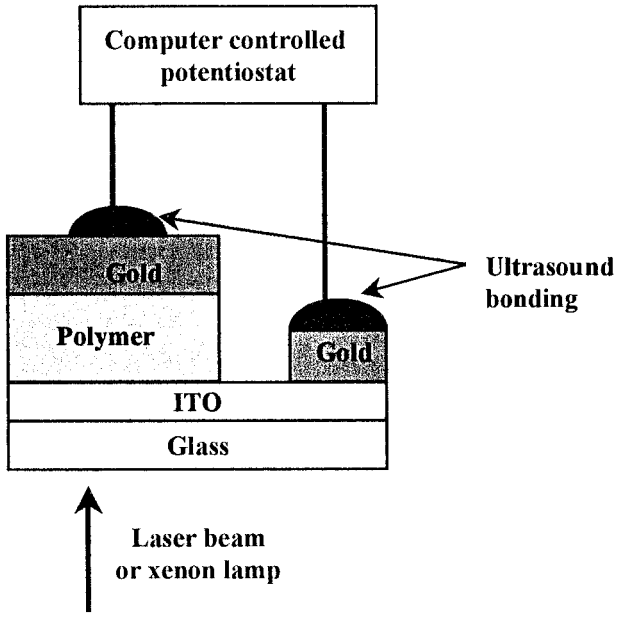

Electrochemical measurements were performed on a homemade computer-controlled cyclic voltammetry apparatus. A three-electrode system was constructed using a saturated calomel reference electrode with LiCl salt bridge and an ITO-coated glass electrode covered with the active polymer layer. Measurements were performed in dry and deoxygenated acetonitrile solutions containing 0.1 M tetraethylammonium perchlorate.

Photoconductivity measurements were performed on an ITO|polymer|gold sandwich type device composed of the active polymer placed between an ITO electrode and a gold electrode, Scheme 1. The same setup was used for all experiments. An argon ion laser (Coherent, Innova 90C, λ_{ex} = 350 and 360 nm) and a xenon lamp (PTI) were used as the optical pump beams for the different experiments. The sample was placed in a temperature-controlled vapor-filled optical chamber for all measurements. A computer-controlled potentiostat was used to follow the different electrical characteristics of the sample.

III. Results and Discussion

III.a. Electrochemical Properties. The electrochemical characteristics of electropolymerized films of p-Pyr-V^{2+}-Me in dry acetonitrile (0.1 M $(Et)_4N^+ClO_4^-$, 100 mV s^{-1}) were similar to earlier reports,[18] with four pseudoreversible redox waves at −0.60 V ($V^{2+/1+}$), −1.07 V ($V^{1+/0}$) and −0.76 V ($V^{0/+1}$), −0.27 V ($V^{1+/2+}$).[19] Cyclic voltammograms of poly(*N*-(3-pyrrol-1-ylpropyl)-4,4′-bipyridinium), at its two protonation states, free base form, p-Pyr-V^+, and protonated form, p-Pyr-V^{2+}-H, are depicted in Figure 1. Clearly, the protonation state of the polymer induces significant changes in the electrochemical properties of the bipyridinium subunits, switching their redox potential from $V < -1.25$ V ($V^{1+/0}$) in the free base state to −0.33 V (V-$H^{2+/1+}$), −0.72 V (V-$H^{1+/0}$), −0.22 V (V-$H^{1+/2+}$), and −0.66 V (V-$H^{0/1+}$)[19] in the protonated film. In the two protonation states, the exact redox peak position and peak to peak separation varied with film thickness and scan rate.

Figure 2a (top curve) displays the differential UV−vis absorption spectrum, ΔOD, of a film of p-Pyr-$V^{\bullet+}$-Me on ITO under a bias of −0.6 V vs SCE. The spectrum features two pairs of absorption peaks denoted M_1, M_2 and D_1, D_2,

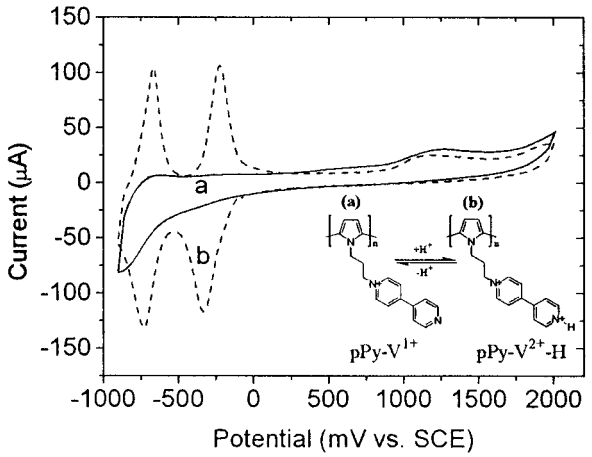

Figure 1. Cyclic voltammograms of poly(*N*-(3-pyrrol-1-ylpropyl)-4,4′-bipyridinium), at its two protonation states: (a) free base form, p-Pyr-V^{+}; (b) protonated form, p-Pyr-V^{2+}-H. Conditions: scan rate = 0.1 V s^{-1}; reference electrode = SCE; electrolyte = 0.1 M tetraethylammonium perchlorate.

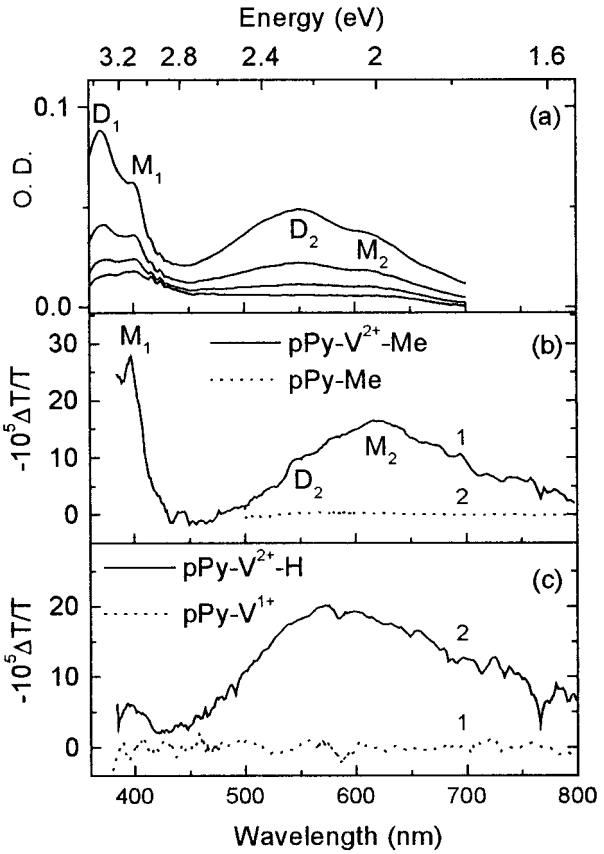

Figure 2. (a) UV−vis absorption spectra of films on ITO at −0.4 V: (top curve) p-Pyr-V^{2+}-Me; (lower curves) monoreduced p-Pyr-V^{2+}-Me at decreasing concentrations of the reduced bipyridinium species. Conditions: reference electrode = SCE; electrolyte = 0.1 M tetraethylammonium perchlorate. The flat bottom curve is the absorption for zero bias. (b) Photoinduced absorption spectra of (1) a film of p-Pyr-V^{2+}-Me and (2) a film of p-Pyr-Me on ITO at zero bias. Conditions: λ_{ex} = 350 and 360 nm; chopper frequency = 140 Hz, T = 294 K. (c) Photoinduced absorption spectra of polymer poly(*N*-(3-pyrrol-1-ylpropyl)-4,4′-bipyridinium): (1) free base form, p-Pyr-V^{+}; (2) protonated form, p-Pyr-V^{2+}-H. Conditions: λ_{ex} = 350 and 360 nm; chopper frequency = 140 Hz, T = 294 K.

respectively. The observed bands M_1 and M_2 (λ_{max} = 400 and 601 nm, respectively) are typical absorption bands of the monomer form of the monoreduced bipyridinium moiety, $V^{\bullet+}$. The observed bands D_1 and D_2 (λ_{max} = 372 and 550 nm, respectively) are similar to the previously reported bands of the spin-paired monoreduced bipyridinium dimer, $[V^{\bullet+}]_2$.[20] The curves in Figure 2a present the differential absorption spectra of the reduced film at different concentrations of the reduced bipyridinium species. The evolution of the dimer bands indicates that monoreduced bipyridinium, p-Pyr-$V^{\bullet+}$-Me, species tend to form aggregates at high local concentrations even in the solid state. Deconvolution of the absorption bands at the 300−400 nm spectral range and using the known extinction coefficients of the D_1 and M_1 bands yielded an equilibrium constant of K_D = 175 ± 10% M^{-1}, assuming the formation of dimers. This value of K_D found in our system is somewhat lower than that found in solutions,[21] possibly due to the higher reorganization energy required for dimerization in the film compared to solutions. We thus conclude that even in the solid state, increasing the concentration of the reduced bipyridinium species results in spin pairing of the $V^{\bullet+}$ units in p-Pyr-$V^{\bullet+}$-Me.[19] A similar aggregation pattern is found in reduced films of p-Pyr-V^{2+}-H.

III.b. Photoinduced Absorption—Evidence for Photoinduced Charge Separation. Figure 2b (solid line) presents the photoinduced absorption spectrum of a film of p-Pyr-V^{2+}-Me on ITO at zero bias. The spectrum contains two bands at 396 and 619 nm that are indicative of the monoreduced form of the bipyridinum subunit. Thus, photoexcitation of p-Pyr-V^{2+}-Me at zero bias leads to charge separation due to electron-transfer from the photoexcited poly(alkylpyrrole) backbone to the bipyridinium electron acceptor subunits. For comparison, the dashed line in Figure 2b presents the photoinduced absorption spectrum of poly(*N*-methylpyrrole) (**4**), p-Pyr-Me, lacking the electron acceptor subunits. The absence of any photoinduced absorption spectrum suggests that p-Pyr-Me is photoinert in the same temporal and spectral range. Similarly, the dashed and solid lines in Figure 2c show the photoinduced absorption spectra of free base p-Pyr-V^{+} and its protonated derivative, p-Pyr-V^{2+}-H, respectively. Free base p-Pyr-V^{+} is photoinert and its photoinduced absorption reveals no evidence for any charge separation products. In contrast, its protonated analogue, p-Pyr-V^{2+}-H, is photoactive, yielding charge-separated states that are similar to those found for p-Pyr-V^{2+}-Me. The difference in photoactivity between free base p-Pyr-V^{+} and its protonated derivative, p-Pyr-V^{2+}-H, is attributed to the difference in the redox properties of the electron acceptor units attached to the polymer backbone, as can be seen from Figure 1. Monoalkyl 4-(4-pyridine) pyridinium groups exhibit only poor electron acceptor properties. Therefore, electron-transfer processes between such systems and photoexcited polypyrrole are ineffective. Protonation of p-Pyr-V^{+} leads to the formation of p-Pyr-V^{2+}-H, having efficient electron acceptor bipyridinium subunits and to an efficient photoinduced charge separation process.

Parts a and b of Figure 3 present the chopper-frequency dependence of the photoinduced absorption signal of p-Pyr-V^{2+}-Me at 395 and 620 nm, respectively. The figures show both the in-phase (solid squares) and out-of-phase (solid circles) components on a log−log scale. Using the frequency at which the out-of-phase signal reaches a maximum,[22] ν_{max}, we determine the characteristic relaxation times for the two bands, $\tau = 2\pi/\nu_{max}$, to be 3 ± 2 ms. The insets in parts a and b of Figure 3 show the laser intensity dependence of the in-phase component at frequencies below and above ν_{max}. For both bands, above ν_{max} the in-phase component is nearly linear with the laser intensity, while below ν_{max} it is close to a square-root depen-

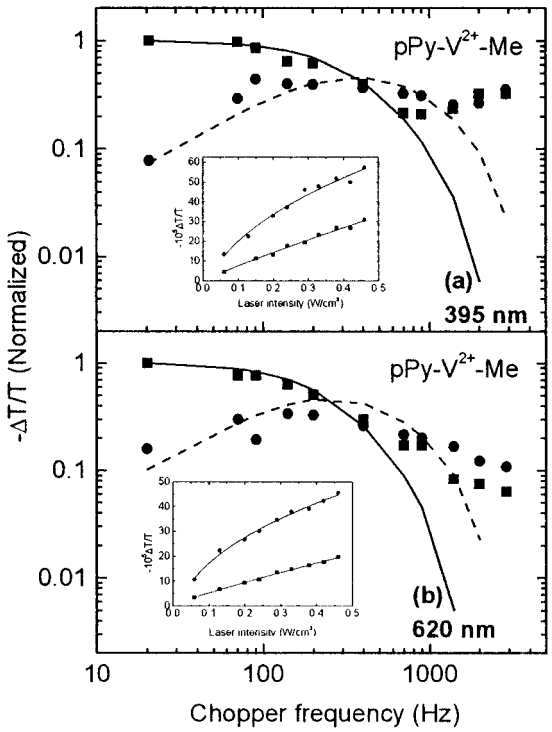

Figure 3. Chopper-frequency dependence of the in-phase (solid squares) and out-of-phase (solid circles) photoinduced absorption signal of p-Pyr-V^{2+}-Me probed at (a) 395 nm and (b) 620 nm. The inset shows the laser intensity dependencies at 20 Hz (solid circles) and 200 Hz (solid squares). Conditions: $\lambda_{ex} = 350$ and 360 nm, $T = 294$ K.

SCHEME 2

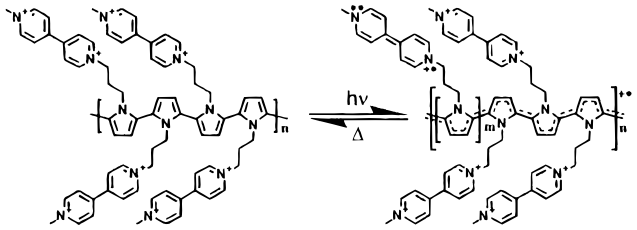

dence. This behavior is characteristic of bimolecular relaxation kinetics[22] described as

$$d[V^{\bullet+}]/dt = G(t) - k_r[V^{\bullet+}]^2 \quad (1)$$

where $[V^{\bullet+}]$ is the concentration of the $V^{\bullet+}$ species, k_r is the bimolecular decay constant, and $G(t) = g(1 + \cos 2\pi\nu t)$ is the generation rate due to the pump laser modulated at frequency ν. The factor g is proportional to the laser intensity and to the quantum efficiency of producing $V^{\bullet+}$. Since the quantum efficiency and the amount of light absorbed by the film were not determined, the fit of eq 1 to the data can yield only the characteristic lifetime defined by $\tau = (gk_r)^{-1/2}$. The values of τ obtained by fitting eq 1 to the data (solid and dashed lines, Figure 3a,b) agree very well with $2\pi/\nu_{max}$ obtained from the maximum of the out-of-phase signal. Note that at the high frequency range the fit deviates from the data, possibly indicating an additional channel for recombination. A more detailed analysis will be published elsewhere.

Scheme 2 summarizes the photoinduced and thermally activated processes in the two systems, as revealed from the different optical and electrochemical experiments. Photoexcited polypyrrole acts as an efficient electron donor in the presence of bipyridinium electron acceptor side groups. Thus, photoexcitation of p-Pyr-V^{2+}-Me results in efficient charge separation. In the absence of appropriate electron acceptors (the case of p-Pyr-V^{+}), photoexcited polypyrrole fails to generate any charge-separated species within its lifetime and decays to its ground state. Electron transfer from photoexcited polypyrrole to bipyridinum species results in the transient photodoping of the conjugated polypyrrole system and formation of reduced bipyridinium species. Both transient redox species, $polypyrrole_{ox}$ and $bipyridinium_{red}$, are expected to contribute to transient photoconductivity.

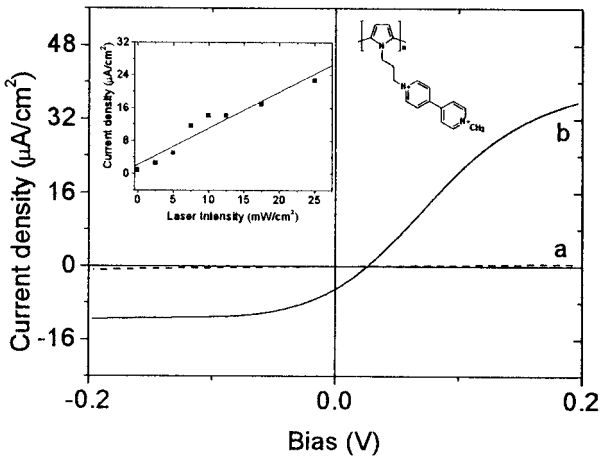

Figure 4. Current voltage curve of an ITO|p-Pyr-V^{2+}-Me|gold sandwich device in the dark (a) and under 7.5 mW cm^{-2} illumination (b). Conditions: $\lambda_{ex} = 350$ and 360 nm; scan rate = 10 mV s^{-1}. Inset: current density measured across the device as a function of light intensity.

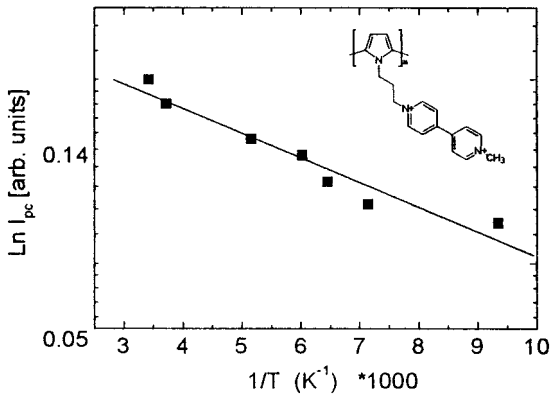

Figure 5. Arrhenius plot of photocurrent as a function of inverse temperature.

III.c. Photoconductivity and Photovoltaic Properties. Figure 4 presents the *I*/*V* characteristics of an ITO|p-Pyr-V^{2+}-Me|gold sandwich device in the dark and under light (7.5 mW·cm^{-2} at $\lambda = 350$ and 360 nm). In the dark, the *I*/*V* curve of the device is linear, having a differential resistance of 530 MΩ in the 0.03 → 0.1 V range. Under light irradiation, the device becomes substantially more conductive and asymmetric with respect to the bias voltage. The resistance drops linearly with increasing light intensity (see inset in Figure 4) and the *I*/*V* curve adopts a nonlinear shape having a differential resistance of 2 MΩ at the 0.03 → 0.1 V range at a laser intensity of 7.5 mW·cm^{-2}. The short-circuit current and open-circuit potential extracted from Figure 4 are 6 μA cm^{-2} (at 7.5 mW·cm^{-2}) and −0.025 V, respectively. Figure 5 presents an Arrhenius plot of the resistivity measured with a light intensity of 25 mW·cm^{-2}. The activation energy extracted from this plot

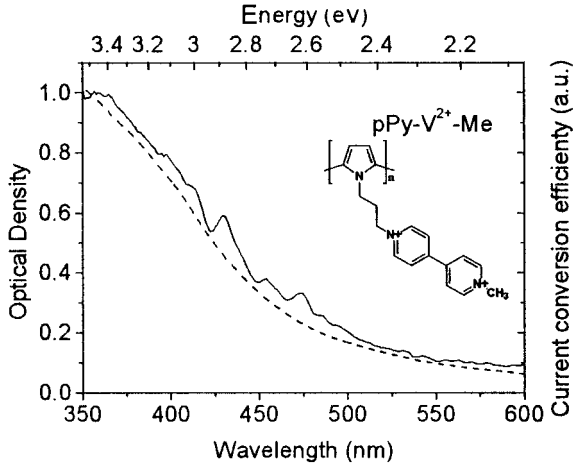

Figure 6. Spectral response of the ITO|p-Pyr-V^{2+}-Me|gold sandwich type device in the UV−visible region (solid line) and absorption spectrum of **2** (dash line).

is 0.57 kcal/mol (0.023 eV), indicative of a charge transport process across a barrier.

Figure 6 depicts the spectral response of the ITO|p-Pyr-V^{2+}-Me|gold sandwich device. The photovoltaic response follows exactly the optical absorption of the films. The quantum yield is typically 0.2%.[23] Films of p-Pyr-V^{2+}-Me and p-Pyr-V^{2+}-H exhibit high stability and could be irradiated for prolonged periods of time without any apparent change in their optical and electrical properties.

IV. Conclusions

Polymers p-Pyr-V^{2+}-Me and p-Pyr-V^{2+}-H, are composed of electron acceptor units anchored to a photoactive conjugated polymer. Upon light illumination, a photodoping process of the type p-Pyr-V^{2+}-R → p-$Pyr^{\bullet+}$-$V^{\bullet+}$-R (R = Me/H**)** takes place, resulting in a long-lived charge-separated species. Charge migration is much faster than the charge recombination process. ITO|p-Pyr-V^{2+}-Me|gold devices exhibit photoconductivity, changing the differential resistance by a factor of 250 at 7.5 $mW{\cdot}cm^{-2}$. ITO|p-Pyr-V^{2+}-Me|gold devices act as plastic photocells, having photon to electron conversion efficiencies of 0.2% in the UV.

The present approach to the preparation of conjugated polymers having pendant electron acceptor groups offers some interesting and unique properties and a possible rational approach to the tuning of material and device properties. The effect of tuning the redox properties of the electron acceptor subunits by the electrooptical properties of polymers of the type of p-*Pyr*-V^{2+}-*R* is currently under investigation.

Acknowledgment. The authors are in debt to Prof. Ch. N. Yarnitzky for his kind help in designing and constructing the cyclic voltammetry apparatus and to Prof. G. Bahir for his kind help with recording the spectral response of the systems. This research was supported partly by the Israel-India cooperation, administered by the Israel Ministry of Science (project number 8985-97), and partly by the European Commission-JOULE-III consortium project (PL971031), and the fund for the promotion of research at Technion.

Supporting Information Available: Synthesis and analytical data for the different monomers and polymers. This material is available free of charge via the Internet at http://pubs.acs.org.

References and Notes

(1) (a) Heeger, A. J.; Diaz-Garcia, M. A. *Curr. Opin. Solid State* **1998**, 16. (b) Hide, F.; Diaz-Garcia, M. A.; Schwartz, B. J.; Heeger, A. J. *Acc. Chem. Res.* **1997**, *30*, 430. (c) See also the following proceedings of the international conferences on synthetic metals held in Seoul Korea **1994** and Snowbird, Utah: *Synth. Met.* **1996**, *69*−*71*, 84−86. (d) Epstein, A. J.; Yang, Y. *MRS Bull.* **1997**, *22*, 13. (e) Epstein, A. J. *MRS Bull.* **1997**, *22*, 16. (f) Wang, Y. Z.; Epstein, A. J. *Acc. Chem. Res.* **1999**, *32*, 217.

(2) (a) Vacar, D.; Dogariu, A.; Heeger, A. J. *Adv. Mater.* **1998**, *10*, 669. (b) Onoda, M.; Tada, K.; Zakhidov, A. A.; Yoshino, K. *Thin Solid Films* **1998**, *76*, 331.

(3) (a) Sariciftci, N. S.; Smilowitz, L.; Heeger, A. J.; Wudl, F. *Science* **1992**, *258*, 1474. (b) Heeger, A. J.; Wudl, F.; Sariciftci, N. S.; Janssen, R. A. J.; Martin, N. *J. Phys. 1* **1996**, *6*, 2151. (c) Janssen, R. A. J.; Moses, D.; Sariciftci, N. S. *J. Chem. Phys.* **1994**, *101*, 9519. (d) Dyakonov, V.; Zoriniants, G.; Scharber, M.; Brabec, C. J.; Janssen, R. A. J.; Hummelen, J. C.; Sariciftci, N. S. *Phys. Rev. B* **1999**, *59*, 8019.

(4) (a) Greenwald, Y.; Cohen, G.; Poplawski, J.; Ehrenfreund, E.; Speiser, S.; Davidov, D. *J. Am. Chem. Soc.* **1996**, *118*, 2980. (b) Sariciftci, N. S.; Mehring, M.; Gaudl, K. U.; Bauerle, P.; Neugebauer, H.; Neckel, A. *J. Chem. Phys.* **1992**, *96*, 7164. (c) Sariciftci, N. S.; Mehring, M.; Gaudl, K. U.; Bauerle, P.; Neugebauer, H.; Neckel, A. *Chem. Phys. Lett.* **1991**, *182*, 326. (d) Bauerle, P.; Gaudl, K. U. *Adv. Mater.* **1990**, *2*, 185.

(5) Janssen, R. A. J.; Christiaans, P. T.; Hare, C.; Martin, N.; Sariciftci, N. S.; Heeger, A. J.; Wudl, F. *J. Chem. Phys.* **1995**, *103*, 8840.

(6) (a) Halls, J. J. M.; Walsh, C. A.; Greenham, N. S.; Marseglia, E. A.; Friend, R. H.; Moratti, S. C.; Holmes, A. B. *Nature* **1995**, *376*, 498. (b) Yu, G.; Heeger, A. J. *J. Appl. Phys.* **1995**, *78*, 4510.

(7) Allemand, M. M.; Koch, A.; Wudl, F.; Rubin, Y.; Diederich, F.; Alvarez, M. M.; Ans, S. J.; Whetten, R. L. *J. Am. Chem. Soc.* **1991**, *113*, 1050.

(8) (a) Roman, L. S.; Anderson, M. R.; Yohannes, T.; Inganas, O. *Adv. Mater.* **1997**, *9*, 1164. (b) Yu, G.; Gao, J.; Hummelen, J. C.; Wudl, F.; Heeger, A. J. *Science* **1995**, *270*, 1789. (c) Brabec, C. J.; Padinger, F.; Sariciftci, N. S.; Hummelen, J. C. *J. Appl. Phys.* **1999**, *85*, 6866.

(9) Kraabel, B.; Hummelen, J. C.; Vacar, D.; Moses, D.; Sariciftci, N. S.; Heeger, A. J.; Wudl, F. *J. Chem. Phys.* **1996**, *104*, 4267.

(10) Bird, C. L.; Kuhn, A. T. *Chem. Soc. Rev.* **1981**, *10*, 49.

(11) (a) Wardman, P. *J. Phys. Chem. Ref. Data* **1989**, *18*, 1637. (b) Willner, I.; Ayalon, A.; Rabinovitz, M. *New J. Chem.* **1990**, *14*, 685.

(12) (a) Adar, E.; Degani, Y.; Goren, Z.; Willner, I. *J. Am. Chem. Soc.* **1986**, *108*, 4696. (b) Yasuda, A.; Mori, H.; Seto, J. *J. Appl. Electrochem.* **1987**, *17*, 567.

(13) (a) Deronzier, A.; Essakalli, M. *J. Phys. Chem.* **1991**, *95*, 1737. (b) Collin, J.-P.; Deronzier, A.; Essakali, M. *J. Phys. Chem.* **1991**, *95*, 5906.

(14) Dalton, E. F.; Murray, W. *J. Phys. Chem.* **1991**, *95*, 6383.

(15) (a) Ramsay, G.; Wolpert, S. M. *Anal. Chem.* **1999**, *72*, 504. (b) Cosnier, S.; Galland, B.; Innocent, C. *J. Electroanal. Chem.* **1997**, *433*, 113.

(16) Bidan, G.; Deronzier, A.; Moutet, J.-C. *J. Chem. Soc., Chem. Commun.* **1984**, 1185.

(17) Eichen, Y.; Nakhmanovich, G.; Gorelik, V.; Epshtein, O.; Poplawski, J. M.; Ehrenfreund, E. *J. Am. Chem. Soc.* **1998**, *120*, 10463.

(18) Lapkowski, M.; Bidan, G. *J. Electroanal. Chem.* **1993**, *362*, 249.

(19) V denotes a bipyridinium moiety and V-H denotes a bipyridinum moiety protonated at one of its nitrogen atoms. The charges of the redox bipyridinium couples, related by the specific electron transfer in question, are given in superscript. Scan rate = 0.1 V s^{-1}.

(20) (a) Stargardt, J. F.; Hawkridge, F. M. *Anal. Chim. Acta* **1983**, *146*, 1. (b) Neta, P.; Richoux, M.-C.; Harriman, A. J. *J. Chem. Soc., Faraday Trans. 2* **1985**, *81*, 1427.

(21) Park, J. W.; Choi, N. H.; Kim, J. H. *J. Phys. Chem.* **1996**, *100*, 769.

(22) Dekel, E.; Ehrenfreund, E.; Gershoni. D.; Boucaud, P.; Sagnes, I.; Campidelli, Y. *Phys. Rev. B* **1997**, *56*, 15734.

(23) The incident photon converted to electron (IPCE) efficiency was calculated according to IPCE% = $I_{SC}/\lambda P_{in}$. See: Roman, L. S.; Mammo, W.; Pettersson, L. A. A.; Andersson, M. R.; Inganas, O. *Adv. Mater.* **1998**, *10*, 774.